Electronic Supplementary Material (ESI) for Journal of Materials Chemistry A.

This journal is © The Royal Society of Chemistry 2022

Electronic Supplementary Information (ESI)

Ultra-Strong, Flame-Retardant, Intrinsically Weldable, and Highly Conductive Metallized Kevlar Fabrics

Xi Lu,[†] Yusheng Ye,[†] Wenhui Shang, Simin Huang, Haifei Wang, Tiansheng Gan, Guokang Chen, Libo Deng, Qixing Wu, Xuechang Zhou*

College of Chemistry and Environmental Engineering

Shenzhen University

Shenzhen 518060, P. R. China

E-mail: xczhou@szu.edu.cn

[†] These authors contributed equally to this work.

The ESI includes:

Figure S1–S18

Table S1–S2

Movie S1–S4

References

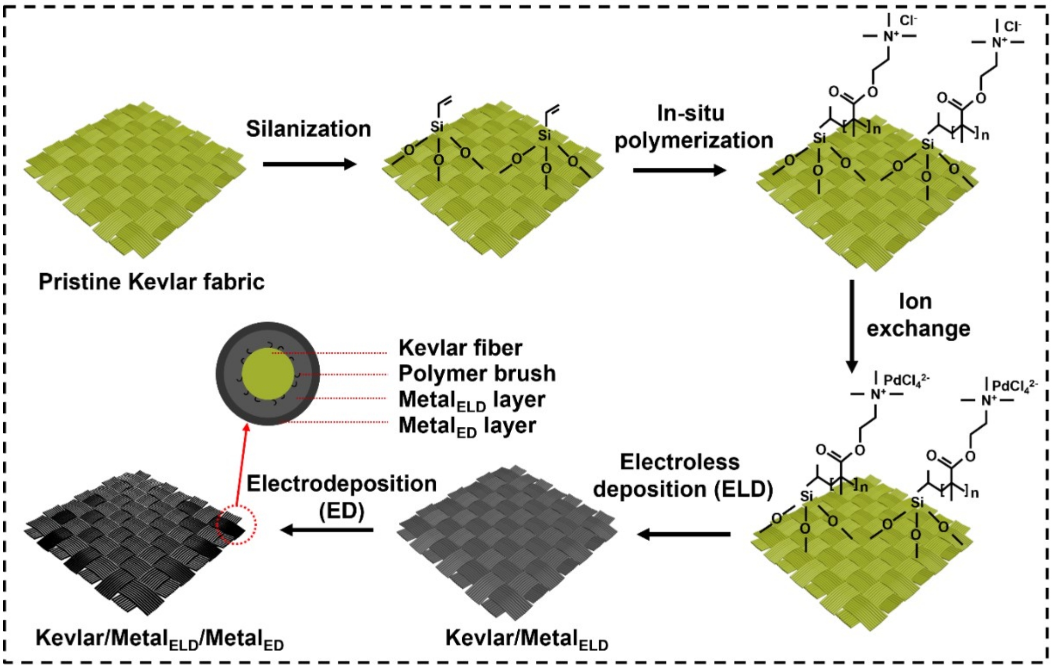

Figure S1. Schematic illustration of the fabrication process of metallized Kevlar fabrics, consisting of polymer-assisted electroless deposition and electrodeposition.

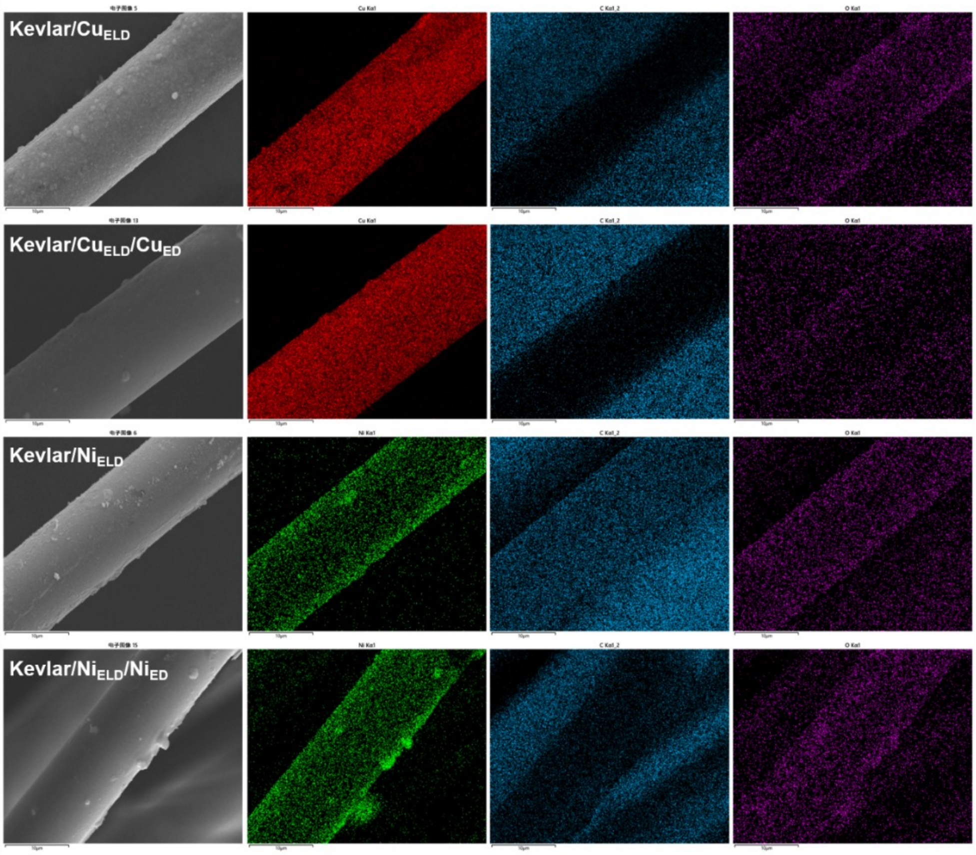

Figure S2. SEM images and EDS analysis of metallized Kevlar fabrics: Kevlar/Cu$_{ELD}$, Kevlar/Cu$_{ELD}$/Cu$_{ED}$, Kevlar/Ni$_{ELD}$, and Kevlar/Ni$_{ELD}$/Ni$_{ED}$.

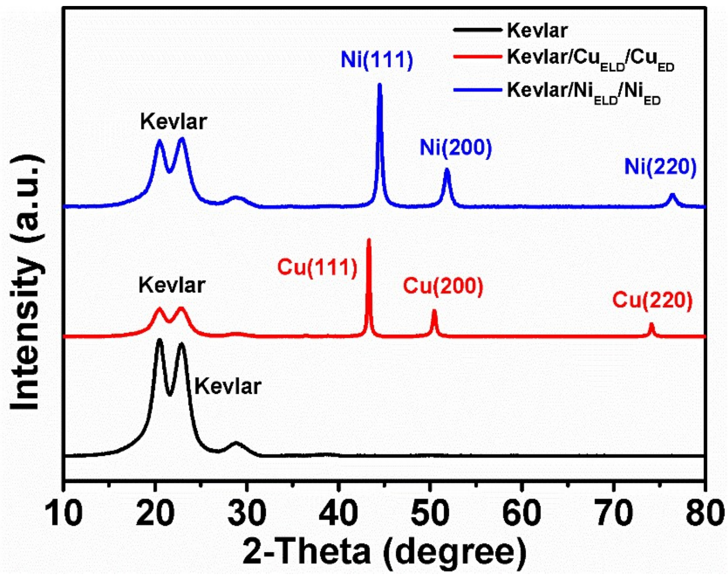

Figure S3. XRD analysis of bare Kevlar fabric and metallized Kevlar fabrics.

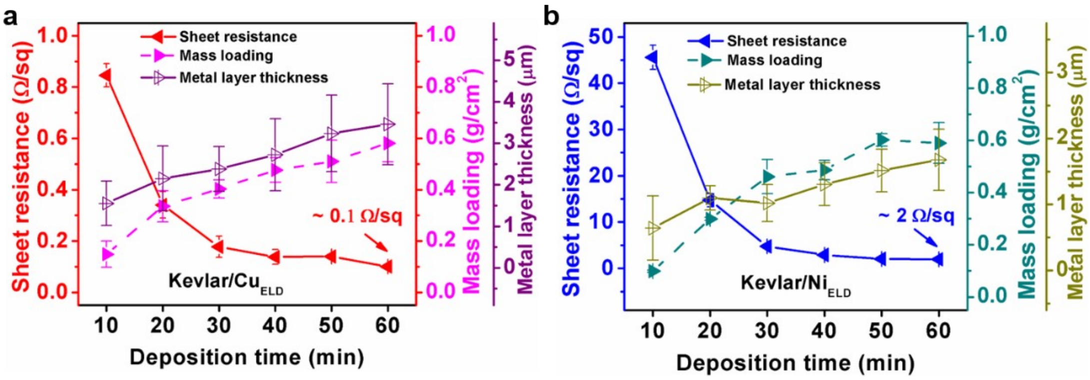

Figure S4. Sheet resistances, mass loadings, and metal layer thicknesses of ELD-based metallized Kevlar fabrics: a) Kevlar/Cu_{ELD} and b) Kevlar/Ni_{ELD}. The thickness of deposited metal layer = (diameter of metallized fiber – diameter of bare fiber) / 2. The diameter of fiber was measured on SEM, and the number of parallel samples is more than five.

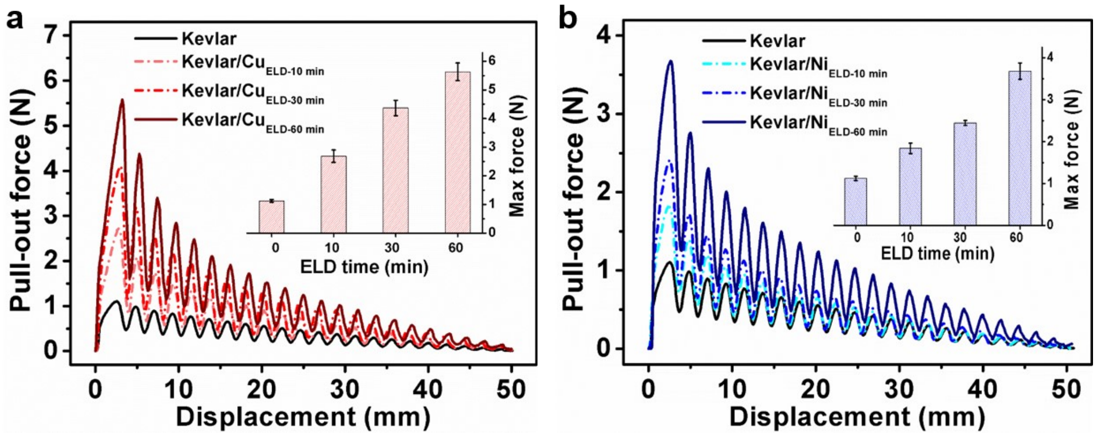

Figure S5. a) Single yarn pull-out test of a) Kevlar/Cu_{ELD} and b) Kevlar/Ni_{ELD} (inset: maximum pull-out force versus ELD time).

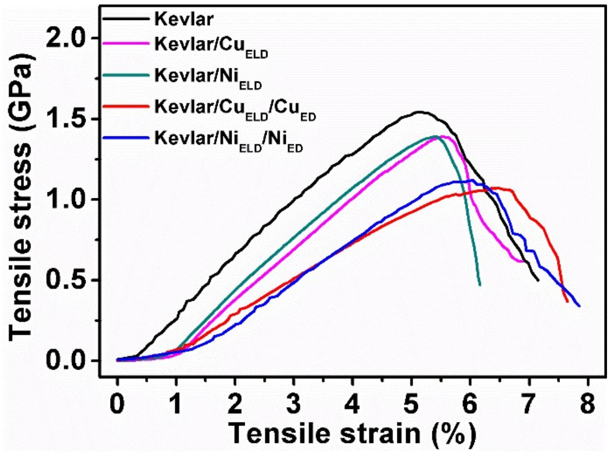

Figure S6. Tensile test of bare Kevlar fabric and metallized Kevlar fabrics.

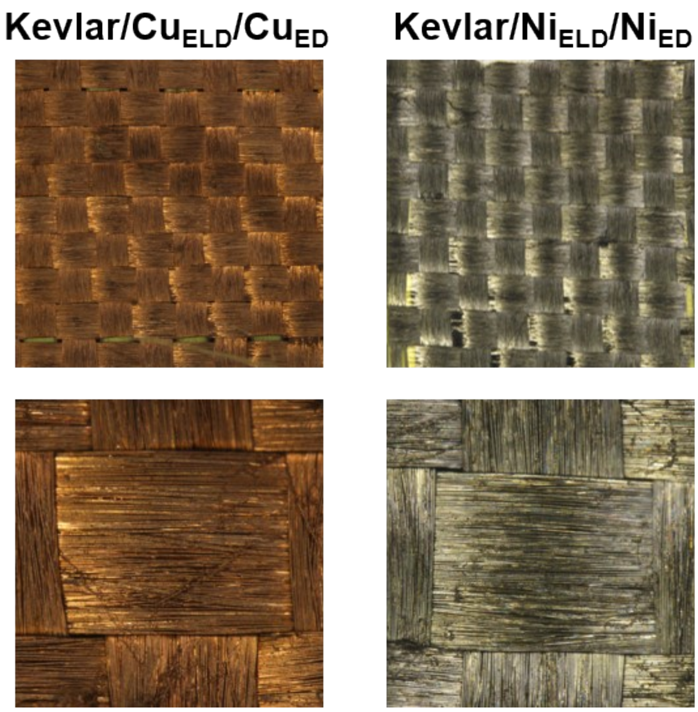

Figure S7. Optical microscope images of metallized Kevlar fabrics after cyclic bending test.

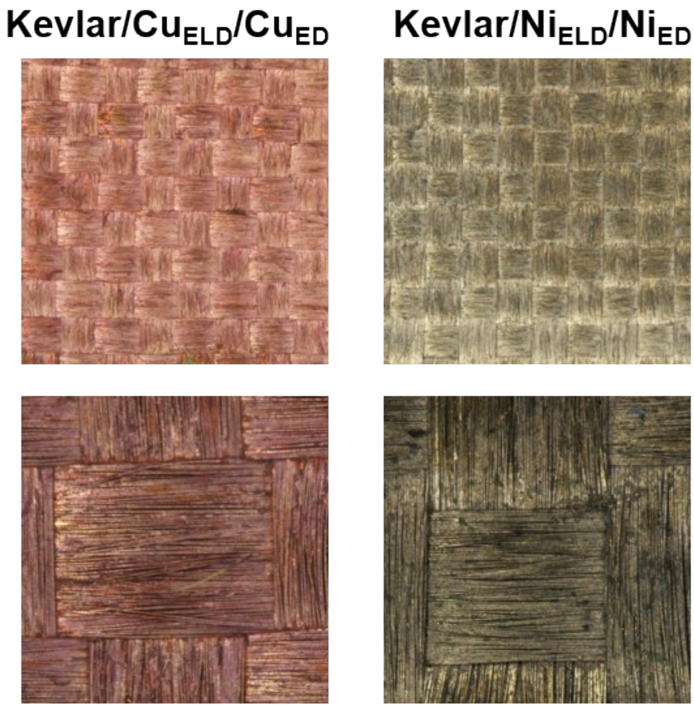

Figure S8. Optical microscope images of metallized Kevlar fabrics after cyclic attach–detach test.

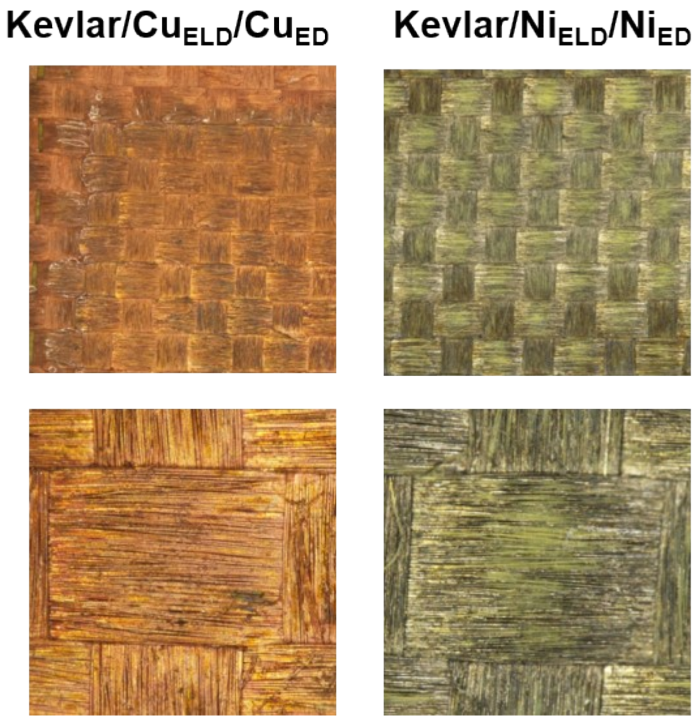

Figure S9. Optical microscope images of metallized Kevlar fabrics after simulated washing test.

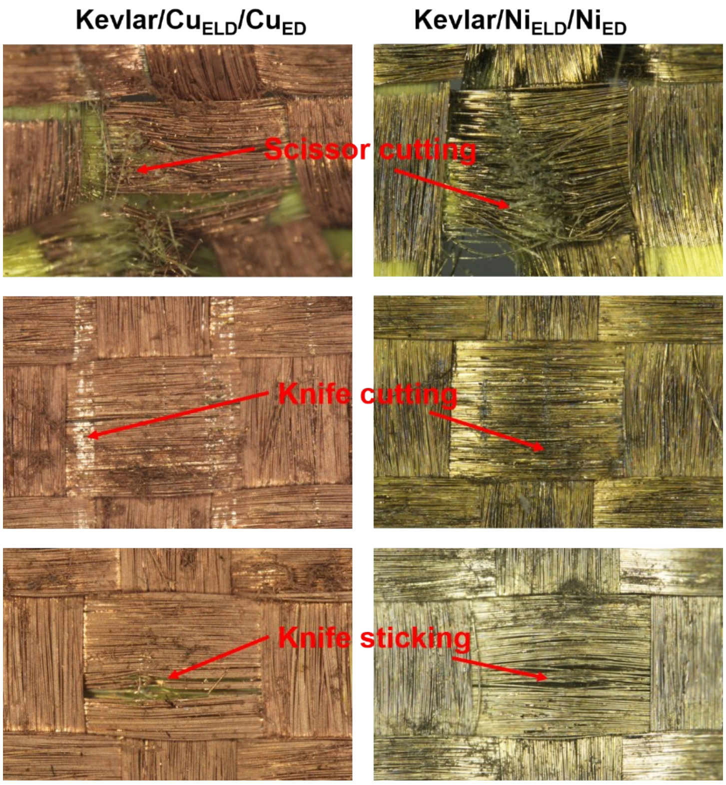

Figure S10. Optical microscope images of metallized Kevlar fabrics after mechanical tortures, i.e., scissor cutting, knife cutting and knife sticking.

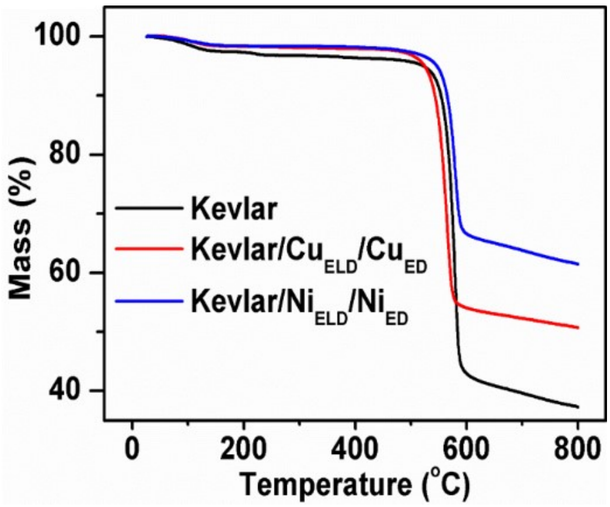

Figure S11. Thermogravimetric analysis (TGA) of neat Kevlar fabric and metallized Kevlar fabrics.

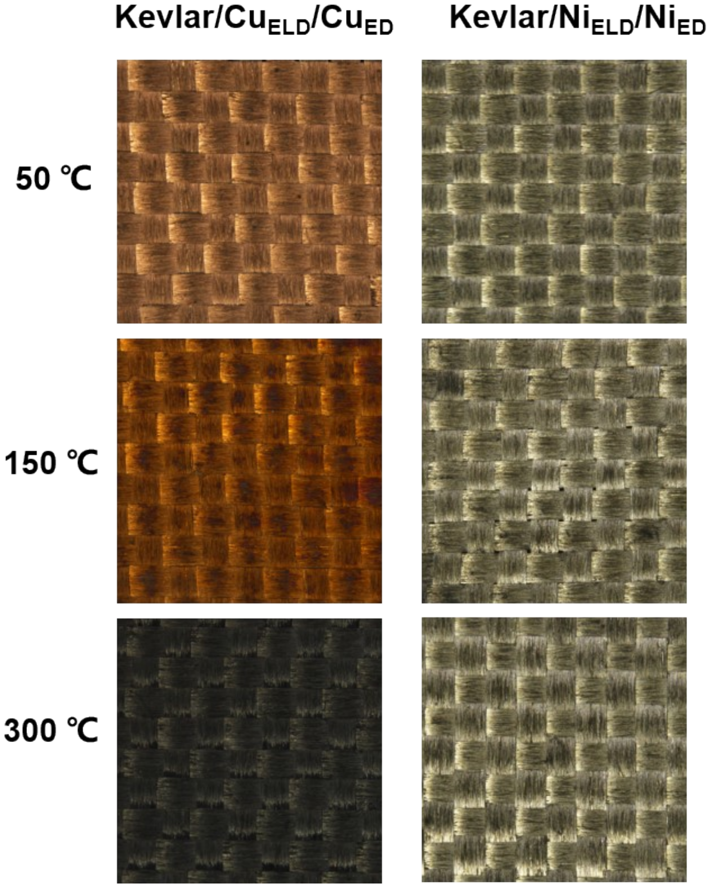

Figure S12. Optical microscope images of metallized Kevlar fabrics after heating treatments at different temperatures (50 °C, 150 °C, and 300 °C) for 1 h.

Figure S13. Control groups, Spandex/Cu$_{ELD}$/Cu$_{ED}$, Kevlar/Cu$_{ELD}$ (with 1.6-μm thickness of metal layer), and Kevlar/Ni$_{ELD}$ (with 0.6-μm thickness of metal layer) failed in the welding process with solder materials.

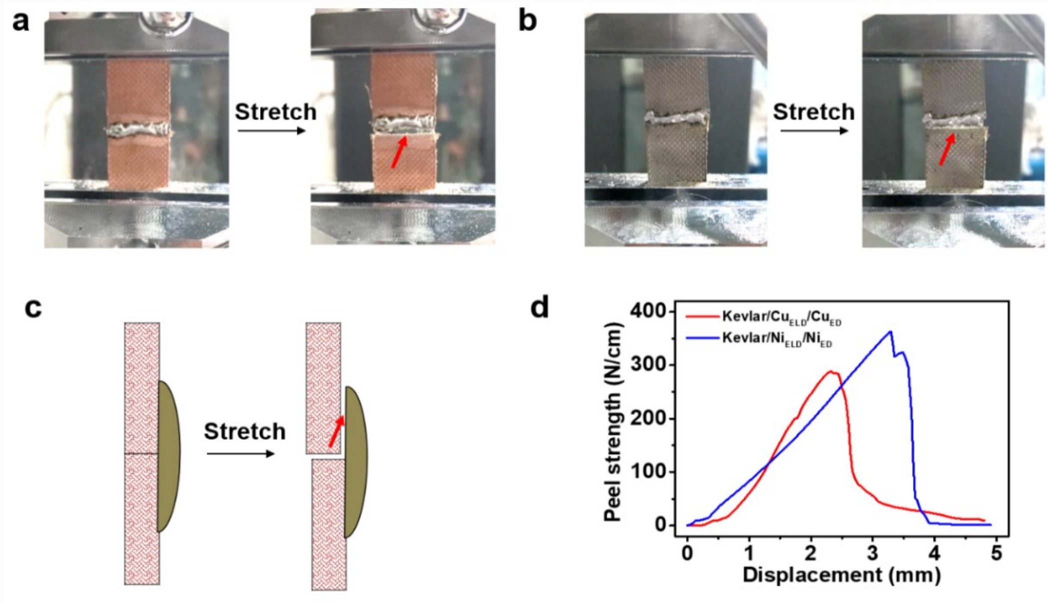

Figure S14. Mechanical properties of MKFs after welded with solders. Tensile tests of welded MKFs: a) Kevlar/Cu_{ELD}/Cu_{ED} and b) Kevlar/Ni_{ELD}/Ni_{ED}. c) Schematic diagram of welded MKF fractured at the interface of deposited metal layer and the solder. d) Curves of peel strength vs displacement of welded MKFs.

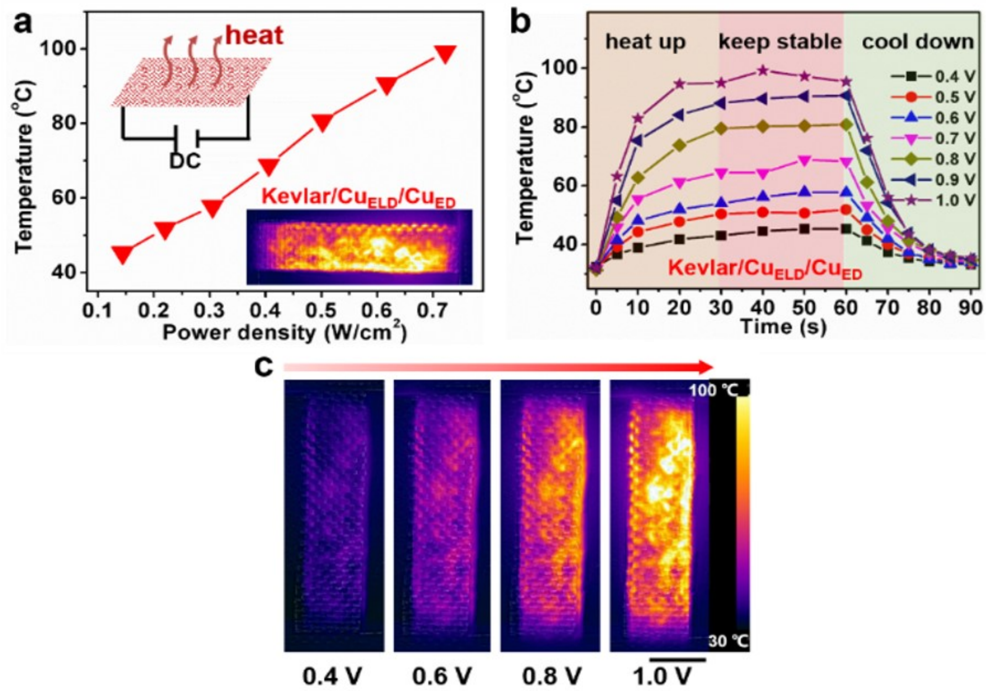

Figure S15. Heater based on Kevlar/Cu_{ELD}/Cu_{ED}. a) Temperature as a function of the input power density. b) Temperature as a function of the time at different applied voltages (0.5–3.0 V). c) IR images of the heater at different applied voltages. Scale bar, 1 cm.

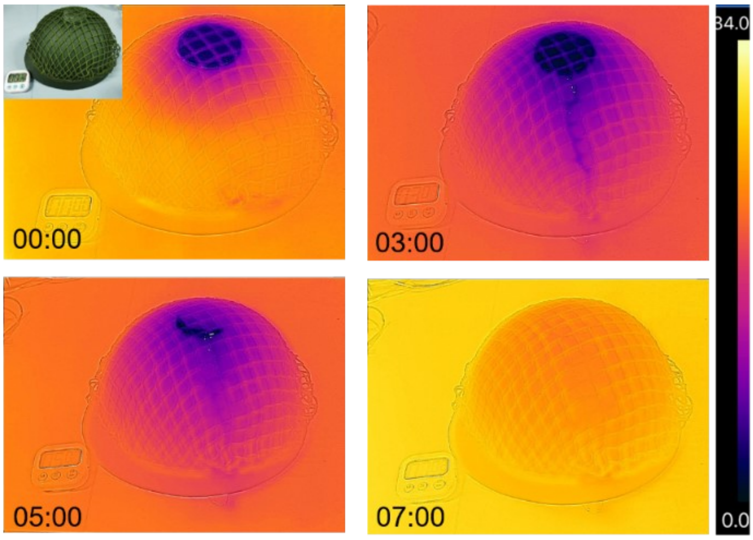

Figure S16. Ice on the helmet naturally melting needs about 7 min. In contrast, MKF-based heater can accelerate the ice melting within 2.5 min, as shown in Figure 4f.

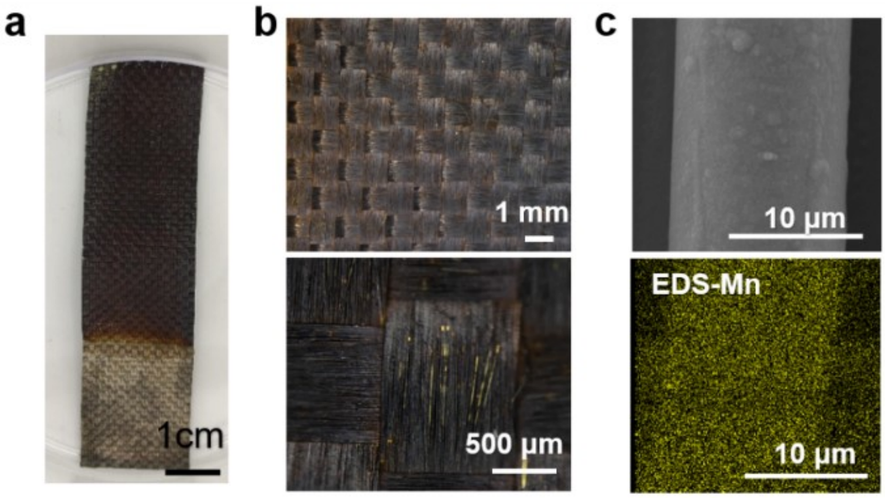

Figure S17. Morphology of SC electrode: Kevlar/Ni_{ELD}/Ni_{ED}/MnO_2. a) Photograph, b) Optical microscope images, and c) SEM image and EDS of manganese element on Kevlar fiber.

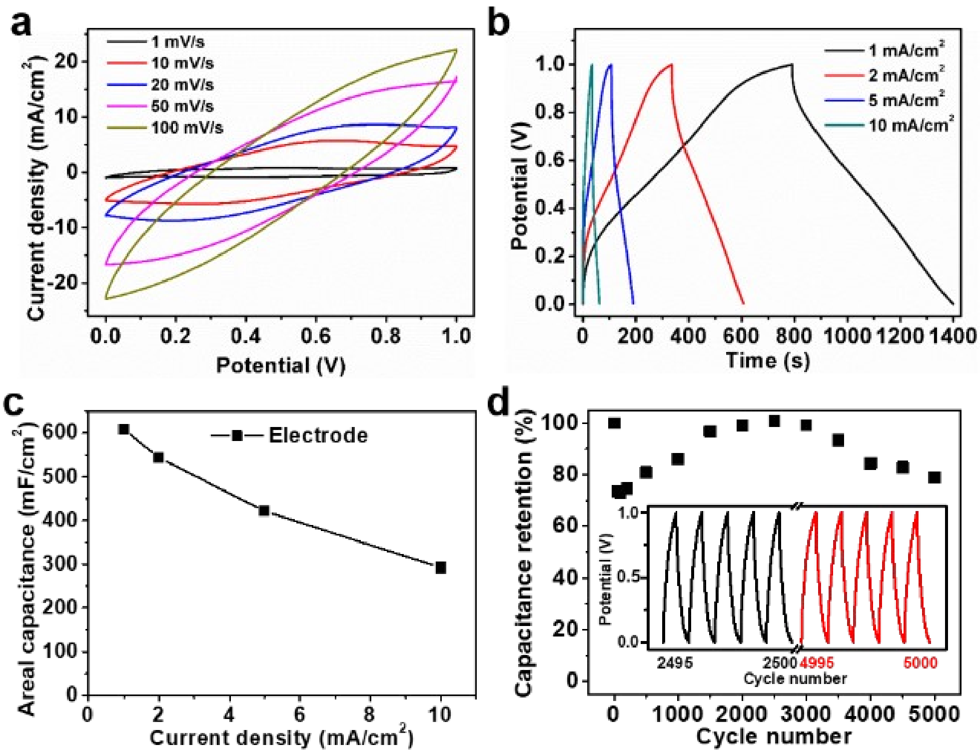

Figure S18. a) CV curves of SC electrode Kevlar/Ni_{ELD}/Ni_{ED}/MnO_2 at different scan rate. b) GCD curves of Kevlar/Ni_{ELD}/Ni_{ED}/MnO_2 at different current density. c) Areal specific capacitance of Kevlar/Ni_{ELD}/Ni_{ED}/MnO_2 at different current density. d) Capacitance retention of supercapacitor device at 10 mA cm^{-2}, inset is the GCD curves of first and last 5 cycles.

Movie S1. MKF-based tough conductor working stably during scissor cutting and knife cutting.

Movie S2. MKF-based wearable heater as knee bands with warming function.

Movie S3. MKF-based flexible heater used to boil up water.

Movie S4. MKF-based supercapacitors operating stably during various torture tests: Scissor cutting, knife cutting, and knife sticking.

Table S1. Comparison of heating performance of fabrics-based flexible heaters.

Textile-based heaters	Voltage (V)	Maximum temperature (°C)	Ref.
Carbonized fabric	4	175	1
Nylon fabric/CuNWs	1.8	143.1	2
CNTs/glucaric acid/chitosan textile	9	149	3
Celluose fabric/MXene	6	100	4
Cotton fabric/MXene	6	150	5
Cotton fabric/rGO/PEDOT:PSS	30	70	6
Cotton fabric/CuNWs/CNT/cellulose	1.8	70	7
Kevlar/Ag@$Ni_xCo_{1-x}Se$/PDMS/rGO	2.1	79	8
Kevlar fabric/MXene/$Fe_xCo_{1-x}P$	3	74	9
Elastomer/CNT textile	8	95	10
PET textiles/PPy/MXene	4	79	11
Silk nanofiber network/CNT	12	65	12
SBS elastomer mesh/AgNWs	1	40	13
Liquid-metal fibre mat	0.48	95	14
Carbonized silk/ceramic composites	10	239	15
Cotton fabric/CNT	40	96	16
Carbon fabric/PDA/ZrO_2	10	60	17
Polyester fabric/carbon black/PU	20	85	18
Spandex fabrics/Cu_{ELD}/Cu_{ED}	3.5	50.5	19
Kevlar/Ni_{ELD}/Ni_{ED}	**3.5**	**296**	**This work**

Table S2. Comparison of tensile strength and areal capacitance of SC electrodes.

SC electrodes	Tensile stress (MPa)	Areal capacitance ($mF\ cm^{-2}$)	Ref.
Aramid Nanofibers/MWCNTs/PANi	158.7	497.3	[20]
PPy/NCFs paper	14.3	1629	[21]
PPy@MnO_2@rGO@Conductive Yarns	700	486	[22]
$Ti_3C_2T_x$ MXene film	32	1380	[23]
	26	1590	
PVA/PEDOT:PSS Hydrogel	9.21	380.8	[24]
PVA/PANi hydrogel	2.4	602	[25]
rGO/MnO_2 paper	8.79	897	[26]
rGO/PPy/cellulose hybrid paper	4.8	1200	[27]
Graphene/WS_2 nanoflake paper	55.7	241.2	[28]
CNT/PPy	16	280	[29]
Graphene/cellulose paper	8.67	81	[30]
Kevlar/Ni_{ELD}/Ni_{ED}/MnO_2	**1000**	**608.9**	**This work**

References

1. M. Zhang, C. Wang, X. Liang, Z. Yin, K. Xia, H. Wang, M. Jian and Y. Zhang, *Adv. Electron. Mater.*, 2017, **3**, 1700193.
2. Z. Guo, C. Sun, J. Zhao, Z. Cai and F. Ge, *Adv. Mater. Interfaces*, 2021, **8**, 2001695.
3. S. Zhu, M. Wang, Z. Qiang, J. Song, Y. Wang, Y. Fan, Z. You, Y. Liao, M. Zhu and C. Ye, *Chem. Eng. J.*, 2021, **406**, 127140.
4. X. Zhao, L.-Y. Wang, C.-Y. Tang, X.-J. Zha, Y. Liu, B.-H. Su, K. Ke, R.-Y. Bao, M.-B. Yang and W. Yang, *ACS Nano*, 2020, **14**, 8793-8805.
5. X. Zhang, X. Wang, Z. Lei, L. Wang, M. Tian, S. Zhu, H. Xiao, X. Tang and L. Qu, *ACS Appl. Mater. Interfaces*, 2020, **12**, 14459-14467.
6. A. Ahmed, M. A. Jalil, M. M. Hossain, M. Moniruzzaman, B. Adak, M. T. Islam, M. S. Parvez and S. Mukhopadhyay, *J. Mater. Chem. C*, 2020, **8**, 16204-16215.
7. Z. Guo, C. Sun, J. Wang, Z. Cai and F. Ge, *ACS Appl. Mater. Interfaces*, 2021, **13**, 8851-8862.
8. A. Hazarika, B. K. Deka, C. Jeong, Y. B. Park and H. W. Park, *Adv. Funct. Mater.*, 2019, **29**, 1903144.
9. A. Hazarika, B. K. Deka, J. Seo, H. E. Jeong, Y.-B. Park and H. W. Park, *Nano Energy*, 2021, **86**, 106042.
10. Y. Li, Z. Zhang, X. Li, J. Zhang, H. Lou, X. Shi, X. Cheng and H. Peng, *J. Mater. Chem. C*, 2017, **5**, 41-46.
11. Q.-W. Wang, H.-B. Zhang, J. Liu, S. Zhao, X. Xie, L. Liu, R. Yang, N. Koratkar and Z.-Z. Yu, *Adv. Funct. Mater.*, 2019, **29**, 1806819.
12. N. Gogurla, Y. Kim, S. Cho, J. Kim and S. Kim, *Adv. Mater.*, 2021, **33**, 2008308.
13. S. Choi, J. Park, W. Hyun, J. Kim, J. Kim, Y. B. Lee, C. Song, H. J. Hwang, J. H. Kim, T. Hyeon and D.-H. Kim, *ACS Nano*, 2015, **9**, 6626-6633.
14. Z. Ma, Q. Huang, Q. Xu, Q. Zhuang, X. Zhao, Y. Yang, H. Qiu, Z. Yang, C. Wang, Y. Chai and Z. Zheng, *Nat. Mater.*, 2021, **20**, 859-868.
15. D. Li, B. Tang, X. Lu, W. Chen, X. Dong, J. Wang and X. Wang, *Composites Part A: Applied Science and Manufacturing*, 2021, **141**, 106237.
16. P. Ilanchezhiyan, A. S. Zakirov, G. M. Kumar, S. U. Yuldashev, H. D. Cho, T. W. Kang and A. T. Mamadalimov, *RSC Adv.*, 2015, **5**, 10697-10702.
17. T. Tian, X. Wei, A. Elhassan, J. Yu, Z. Li and B. Ding, *Chem. Eng. J.*, 2021, **417**, 128114.
18. L. R. Pahalagedara, Induni W. Siriwardane, N. D. Tissera, R. N. Wijesena and K. M. N. de Silva, *RSC Adv.*, 2017, **7**, 19174-19180.
19. X. Lu, W. Shang, G. Chen, H. Wang, P. Tan, X. Deng, H. Song, Z. Xu, J. Huang and X. Zhou, *ACS Appl. Electron. Mater.*, 2021, **3**, 1477-1488.
20. X. Zhan, Q. Yin, W. Mai, Y. Wang, A. F. A. A. Melo, K. Jiang, H. Jia and Q. Ji, *J. Electrochem. Soc.*, 2021, **168**, 020513.
21. Z. Wang, D. O. Carlsson, P. Tammela, K. Hua, P. Zhang, L. Nyholm and M. Strømme, *ACS Nano*, 2015, **9**, 7563-7571.
22. Y. Huang, H. Hu, Y. Huang, M. Zhu, W. Meng, C. Liu, Z. Pei, C. Hao, Z. Wang and C. Zhi, *ACS Nano*, 2015, **9**, 4766-4775.
23. X. Zhao, Z. Wang, J. Dong, T. Huang, Q. Zhang and L. Zhang, *J. Power Sources*,

2020, **470**, 228356.
24. Q. Liu, J. Qiu, C. Yang, L. Zang, G. Zhang and E. Sakai, *Adv. Mater. Technol.*, 2021, **6**, 2000919.
25. Y. Zou, C. Chen, Y. Sun, S. Gan, L. Dong, J. Zhao and J. Rong, *Chem. Eng. J.*, 2021, **418**, 128616.
26. A. Sumboja, C. Y. Foo, X. Wang and P. S. Lee, *Adv. Mater.*, 2013, **25**, 2809-2815.
27. C. Wan, Y. Jiao and J. Li, *J. Mater. Chem. A*, 2017, **5**, 3819-3831.
28. J. Li, K. Liao, X. Wang, P. Shi, J. Fan, Q. Xu and Y. Min, *Adv. Mater. Interfaces*, 2017, **4**, 1700419.
29. Y. Chen, L. Du, P. Yang, P. Sun, X. Yu and W. Mai, *J. Power Sources*, 2015, **287**, 68-74.
30. Z. Weng, Y. Su, D.-W. Wang, F. Li, J. Du and H.-M. Cheng, *Adv. Energy Mater.*, 2011, **1**, 917-922.